Journal of Shellfish Research, Vol. 24, No. 4, 1161–1168, 2005.

ANALYSIS OF CHROMOSOMAL DNA CONTENT IN PACIFIC RED ABALONE *HALIOTIS RUFESCENS* BY FLUORESCENCE IMAGE ANALYSIS

CRISTIAN GALLARDO-ESCÁRATE,[1,2]* JOSUÉ ÁLVAREZ-BORREGO,[2] MIGUEL ÁNGEL DEL RÍO-PORTILLA,[3] ELISABETH VON BRAND-SKOPNIK[1] AND MARIO A. BUENO[2]

[1]*Departamento de Biología Marina, Facultad de Ciencias del Mar, Universidad Católica del Norte. Larrondo 1281, Casilla 117, Coquimbo, Chile;* [2]*Dirección de Telemática,* [3]*Departamento de Acuicultura. Centro de Investigación Científica y de Educación Superior de Ensenada. Km. 107 Carretera Tijuana–Ensenada, Código Postal 22860, Ensenada, B.C. México*

ABSTRACT The fluorescence fading and chromosome imaging method were used together to analyze chromosomal DNA contents (haploid set) in Pacific red abalone *Haliotis rufescens* (Archaeogastropoda: Haliotidae). The fluorescence intensity was measured each 1.6 sec in *H. rufescens* chromosomes (2 n = 36) stained with DAPI. The fluorescence of each chromosomal type was recorded using color digital images of 24 bits. These kind of images allowed converting the RGB (true color) images to pseudocolor images to quantify the fluorescence intensity by means of 256 levels of brightness. Algorithms built with MATLAB software were used to determine the area under the curve (fading function). Therefore, estimates of DNA contents in individual chromosome types were obtained. Their DNA contents were related with chromosomal sizes ($P < 0.001$). The DNA values found showed a range from 0.1106 ± 0.0045 pg (chromosome # 1) to 0.0890 ± 0.0060 pg (chromosome # 18). The genome size calculated for *H. rufescens* by sum of all chromosomal DNA contents was 1.77 ± 0.005 pg. This study describes an alternative imaging method to analyze the chromosome morphology and chromosomal DNA contents in molluscs, and represents an alternative approach to the lack of cell lines required in flow cytogenetics.

KEY WORDS: genome size, chromosome image analysis, fluorescence fading, *Haliotis rufescens*, abalone

INTRODUCTION

The Pacific red abalone *Haliotis rufescens* (Swainson 1822) is a marine gastropod inhabiting rocky substrates together with kelp along the Pacific coast from Southern Oregon to Northern California in the United States to the Baja California Peninsula in Mexico (Lindberg 1992). Abalones are economically important marine gastropods that reach moderate to high prices in the world market (Oakes & Ponte 1996), and aquaculture production of red abalone began during the last decade in Mexico. The whole life cycle is managed under controlled conditions. Because of its economical importance, several studies of ploidy manipulation have been carried out to enhance the production of different abalone species (Arai & Wilkins 1986, Fujino et al. 1987, Kudo et al. 1991, Zhang et al. 1998, Maldonado et al. 2001). However, the knowledge on abalone cytogenetic characteristics is sparse.

Modern cytogenetic methods such as chromosome banding and fluorescent *in situ* hybridization (FISH) proved to be useful in understanding the genomic organization of numerous vertebrate species (Gray et al. 2002). The same methods have sporadically been used to examine the chromosome in the phylum Mollusca (Guo & Allen 1997, Zhang et al. 1999b). In particular, available karyologic data on the class Gastropoda indicate that more than 300 species have been analyzed cytogenetically (Patterson 1969, Nakamura 1985, Thiriot-Quiévreux 1994)), whereas <20 of them have been examined using these techniques (Vitturi et al. 2002). In this context, to ascertain the cytogenetic characteristics of *H. rufescens*, the karyotype of this species (2 n = 36) has been reported with eight metacentric, eight submetacentric, one submetacentric/metacentric and one subtelocentric chromosome pair (Gallardo-Escárate et al. 2004, Gallardo-Escárate et al. 2005a).

Together with banding and FISH techniques, flow cytometry has been used for the analysis of DNA contents of genomes, specific chromosomes and chromosomal karyotyping (Langlois et al. 1982, Rodriguez-Juiz et al. 1996, Lucretti & Dolezel 1997, Dolezel et al. 2004). In addition, flow cytometry can be used for the isolation of specific chromosomes for the construction of chromosome-specific libraries, and for gene cloning from a chromosomal-specific region of a complex genome (Macas et al. 1993). However, the application of flow cytometry and sorting (flow cytogenetics) has been used mainly in plant (Dolezel et al. 2004) and human genomes (Trask 2002). The application of these techniques in molluscs has been delayed by difficulties in obtaining cellular line cultures, therefore preparation of suspensions of intact chromosomes and discrimination of individual chromosome types by cytometry remains in stand by until now.

Recently, image analysis methods have been introduced in cytogenetic research (Kato & Fukui 1998, Zhang et al. 1999a, Houtsmuller et al. 2000). It has been shown that the genome size data obtained by image analysis methods are comparable to flow cytometry data (Uozu et al. 1997). We also reported a new method for the estimation of cell DNA content using fluorescence fading (Gallardo-Escárate et al. 2005b). We measured the fluorescence intensity in DAPI-stained nuclei of several species. The estimation of the area under the curve (integral fading) during a fading period was related with the genome size. Our results showed that the fluorescence in spermatozoa and red blood cell nuclei of *Oreochromis mossambicus*, spermatozoa of *Haliotis rufescens* and red blood cell nuclei of *Oncorhynchus mykiss*, decreases rapidly when these nuclei were exposed to ultra violet light. The integral fading values calculated for each nuclear type showed a linear relationship with genome size reported for these species (r = 0.99), therefore we proposed a linear equation ($\hat{y} = 3337.2\hat{x} + 596.8$) to estimate other genome size. This work demonstrated the feasibility to estimate genome sizes by quantification of fluorescence fading.

In this study, we analyzed chromosomal DNA contents and

*Corresponding author: cgallard@ucn.cl

their DNA variations. Furthermore, to propose chromosomes as markers in *Haliotis rufescens* we analyzed the correlations among DNA contents measured by fluorescence image analysis, and chromosome areas and lengths. Finally, we proposed an alternate technique for DNA content estimation in abalone chromosomes using image analysis.

MATERIALS AND METHODS

Chromosome Preparation and DNA-fluorescent Staining

Swimming trochophore larvae of Pacific red abalone (20–24 h after fertilization), were placed in a colchicine seawater solution (0.005%) during 3 h. After the antimitotic treatment, the samples were kept for 45 min in a hypotonic solution (seawater: distilled water, 1:1). The larvae were fixed in modified Carnoy solution (methanol: acetic acid, 3:1) by rinsing the samples three times in the fixative at 10 min intervals. Fixed cells were stored at 4°C in 70% ethanol solution. The cell suspension of each sample was made by cell dissociation in 50% acetic acid and strong agitation with a Pasteur pipette. The cell suspension was then dropped onto preheated glass slides (45°C) and air-dried. Then slides were washed in three changes with Phosphate Buffer Saline (13 mM NaCl, 0.2 mM KCl, 0.8 mM Na2HPO4, 0.2 mM KH2PO4, pH 7.4) (PBS1X) for 5 min each time, and incubated with DAPI solution in the dark for 25 min at room temperature (25°C) using a Coplin jar. The DAPI solution stain was prepared with 4,6-diamidino-2-phenylindole (DAPI) (Sigma–Aldrich, USA) in PBS1X at 0.5 μg/mL. Slides were then observed only with PBS1X, none antifading was used.

Image Capture

The image capture was generated by programming the digital capture process using QWIN software (Copyright by Imaging Systems Ltd, Cambridge, United Kingdom 1997). This program captured a color digital image of 2088 × 1550 pixels. For each observation field, images were captured in intervals of 1.6 sec during a fluorescence-fading period in the same field. The aim of these sequential image capturing was to obtain images to be used for chromosomal fluorescence fading estimation, and chromosome morphologic measurements. The image capture conditions were: CCD exposure time of 209 milliseconds, gamma equal to 1 (linear response) and color depth of 8 bit/channel. The fluorescence was measured using a motorized epifluorescent microscope (Leica model DMRXA2) equipped with a RGB color digital camera of 36-bits and 3.3 Mega Pixels (Leica model DC300).The fluorescence conditions were: excitation filter UV 340–380 nm, dichromatic mirror DM 400 nm, suppression filter LP 425, absorption band AB 435–485 nm and objective lens PL Fluotar 100X/1.3.

Chromosome Sorting

Identification of homologue chromosomes was performed by digital measurements according to (Gallardo-Escárate et al. 2004). After identification of homologue chromosomes, determinations of chromosomal arm lengths (short and large) and chromosome areas were determined using Image ProPlus software version 4.0 (Copyright 1993–1998 Media Cybernetics). A total of 356 chromosomes were randomly measured and their centromeric index was calculated (100 × length of short arm/total chromosome length). Karyotype was arranged, and classified according to (Levan et al. 1964) by decreasing size and centromeric position.

Fluorescence Fading Analysis

The image analysis was performed by three algorithms specifically built using MATLAB software (Copyright 1984–2000, The MathWorks, Inc.). The first algorithm was built to obtain subimages of 51 × 51 pixels from the initial captured images of 2088 × 1550 pixels. Each subimage of 51 × 51 pixels contained a single chromosome, which was captured during the fading period. The fluorescence fading period was recorded in a stack of 20 images (fading period). The second algorithm was used to generate a binary mask or a contour of the chromosome. The purpose of this mask was to filter the image background by multiplication between pseudocolor image and binary mask (0 and 1 pixel values), to obtain the highest brightness information (fluorescence) from each chromosome image. The third algorithm was generated to estimate the area under the curve by one integration function of the pixel intensities (fluorescence intensity) in 256 level of brightness, thus for each chromosome DNA-fluorescent mean intensity in a 256 scale was calculated. The pixel mean intensity (*PMI*) was estimated using the binary mask on the fluorescent image of each chromosome type. Each chromosome image was measured during the fluorescence-fading period until the fading time was completed. If all *PMI* are plotted during a fluorescent fading period, the area under the curve represents the integral fading (*IF*) like:

$$IF = \sum_{i=1}^{n} (PMI)_i * \Delta t \qquad (1)$$

where i represents the number of images in a fading period and Δt time among each image captured. Thus *IF* represents the integral fading by the sum of the mean intensity (fluorescence) during the fading period. The haploid value of each chromosome was obtained by the linear model built with standard C-values. Using the linear model equation $\hat{y} = 3337.2\hat{x} + 596.8$, we obtained the unknown chromosomal DNA content for each chromosome type from the *IF* value estimated by quantification of fluorescence fading. To obtain the value of haploid chromosomal DNA content, the value of the bivalent chromosome was divided by two.

Statistical Analysis

To obtain the chromosomal DNA content variations, several analyses were carried out to estimate the percentage of chromosomal variation and their contribution to the total genome size variation. These calculations were performed using 1-way ANOVA and a *posteriori* Tukey HSD test. The ANOVA assumptions, normal distribution and homogeneity of variances were tested using Kolmogorov-Smirnov test and Bartlett test respectively. The statistical analyses were carried out using Statistica 6.1 software (Copyright 1984–2002, StatSoft, Inc.).

RESULTS

Chromosomal Fluorescence Fading

All chromosomal images in this study were processed using image analysis. The karyological observations on larvae of Pacific red abalone showed a diploid number equal to 36 chromosomes. The karyotype of *Haliotis rufescens* indicated that this species possessed 8 metacentric pairs (1, 3, 6, 7, 14, 15, 17 and 18), 8 submetacentric pairs (2, 4, 5, 8, 9, 10, 11 and 13), 1 (12) was classified as a submetacentric/ metacentric chromosome and one of subtelocentric chromosomes (16) (Fig. 1).

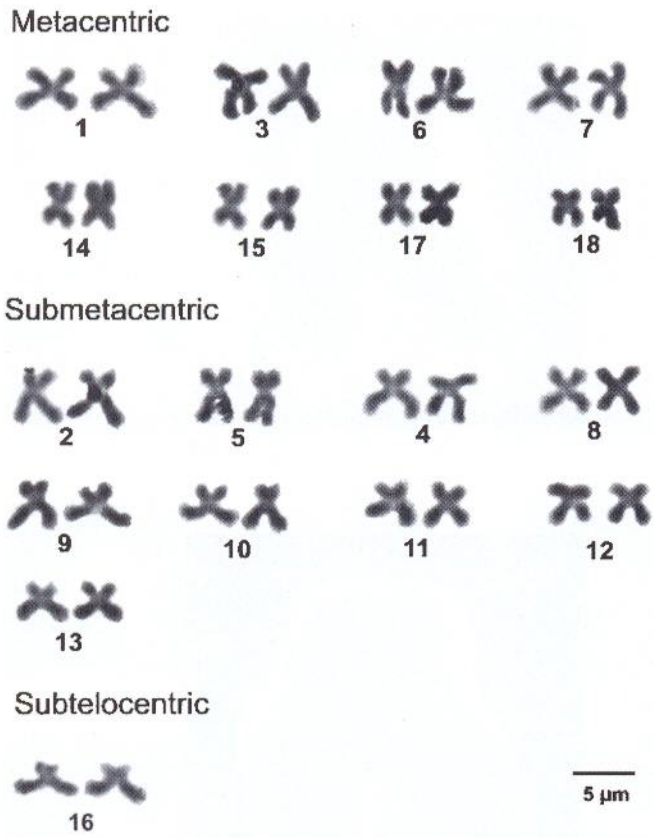

Figure 1. Karyotype of *Haliotis rufescens* obtained from trochophore larvae with 2 n = 36.

The brightness in DAPI-stained chromosomes was analyzed to determine the fluorescence intensity. The fluorescence images of *H. rufescens* chromosomes, recorded in color digital images of 8 bits, allowed converting the RGB (true color) images to pseudocolor images. The pseudocolor image allows visualizing and quantifying the fluorescence intensity by means of 256 levels of brightness (Fig. 2a, 2b). Furthermore, the fluorescence intensity was measured in a subimage of 51 × 51 pixels obtained from initial images of 2088 × 1550 pixels.

In this study we used the fluorescence fading to estimate the DNA content in chromosomes of *H. rufescens*. First, chromosome images (subimages) were digitally measured to classify all captured chromosomes. Figure 3a shows the measurements in both, large and short arms. The fluorescent image was transformed to pseudocolor in reference to fluorescence intensity or 256 brightness levels (Fig. 3b). To discriminate the background, a chromosomal binary mask was built around the chromosome edge. Mask application on the pseudocolor images allowed discrimination of chromosomal regions from the background field (Fig. 3c). The region of interest was obtained by multiplication between (b) and (c) images (Fig. 3d).

To demonstrate the fluorescence fading in single chromosomes, we built a sequence of images from the initial exposures to ultraviolet light until its complete blanching (Fig. 4). The Profile of fading function was generated by fluorescence intensity quantification (Eq. 1). The Figure 5 shows a fading profile in the chromosomes 16 of *H. rufescens*. The fluorescence intensity was highest in the first seconds, after that fluorescence decreased until its total blanching. The area under the curve is proportional to chromosomal DNA content.

Chromosomal DNA Contents

According to the linear model used ($\hat{y} = 3337.2\hat{x} + 596.8$), where $\hat{y}$ represents the integral fading value (*IF*) and $\hat{x}$ the DNA content, we determined the chromosomal DNA content for each chromosome using the fluorescence fading information obtained from the stack of fluorescence images. The DNA content calculated for each chromosome type is shown in Table 1. The highest DNA content was found in the chromosome pair 1, and the lowest DNA content was found in the chromosome pair 18. To determine the base pair content for each chromosome, we assumed that the

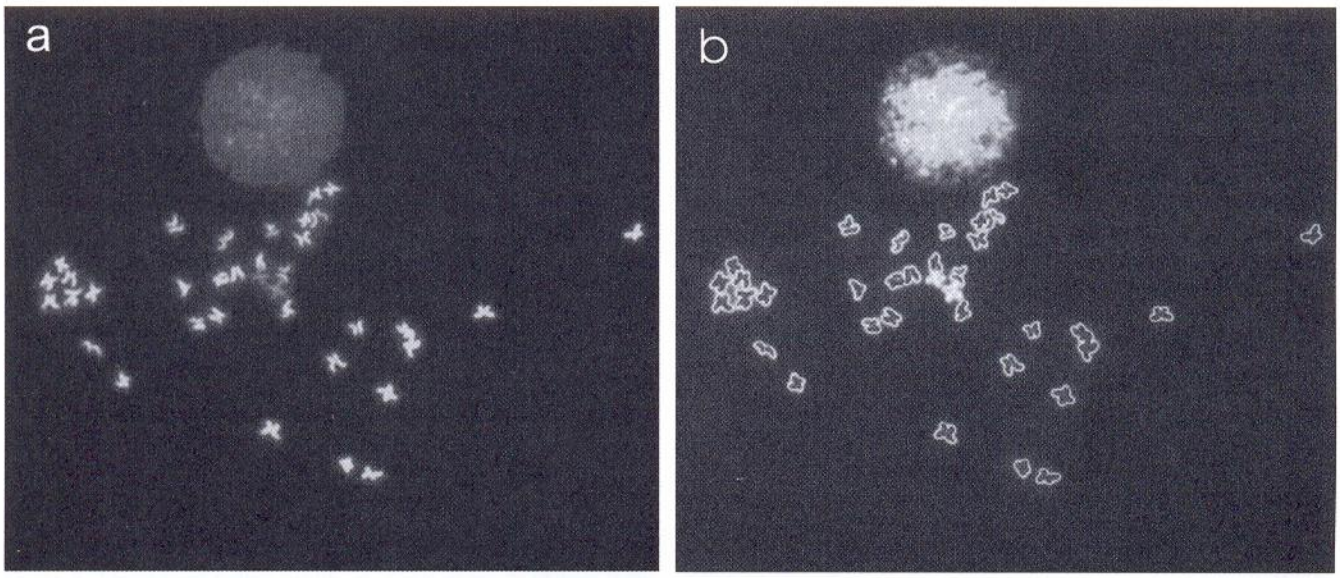

Figure 2. Digital image of a metaphase spread in *Haliotis rufescens*. (a) Metaphase chromosomes stained with DAPI. (b) Digital image obtained by conversion of fluorescence information into pseudocolor (0–255 level of brightness).

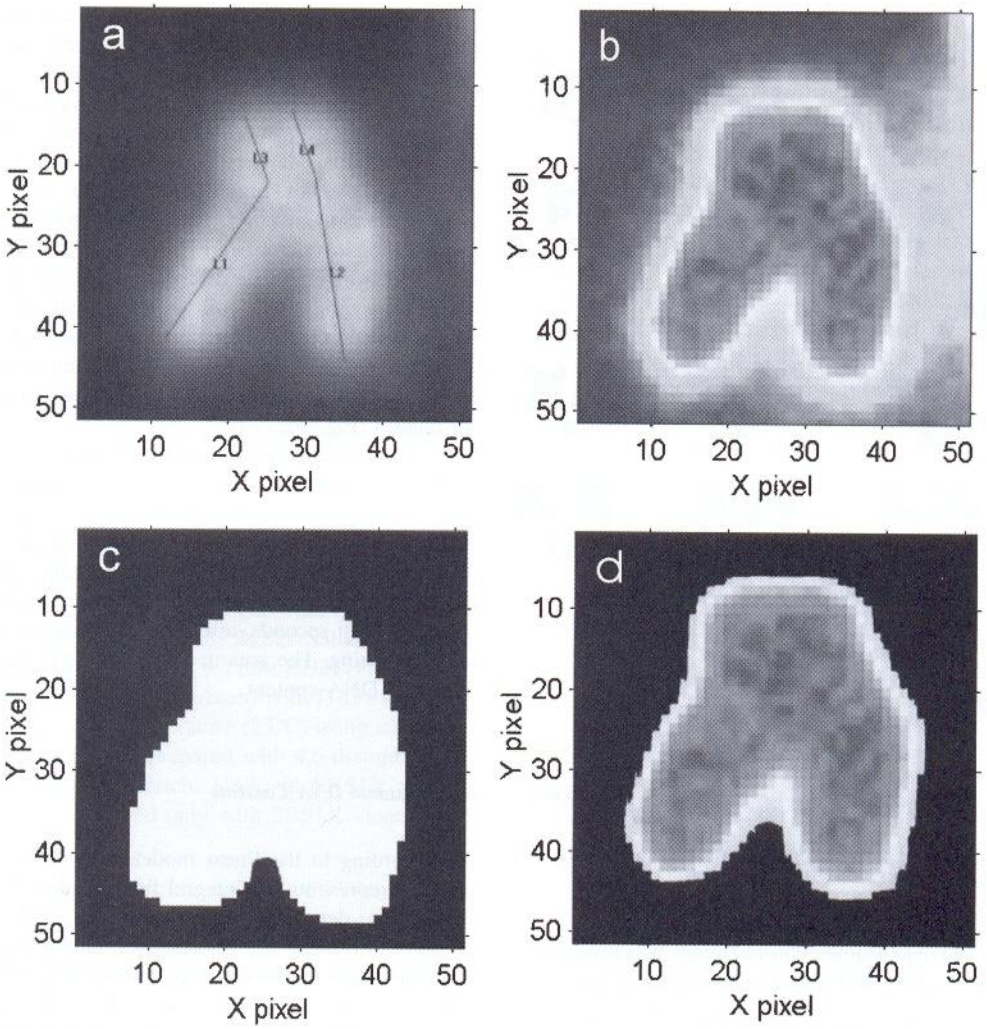

Figure 3. Representative steps of the image manipulation for estimation of fluorescence fading in single chromosomes. (a) Chromosomal measurements. (b) Pseudocolor image in reference to fluorescence intensity. (c) Chromosomal binary mask built from the chromosome edge. (d) The chromosomal regions were discriminated from the background field by the mask built from the chromosomal edge. The region of interest was obtained multiplying the (b) and (c) images.

number of base pairs is equivalent to the mass in picograms (pg) $\times$ 0.978 $\times$ 10^9 bp (Dolezel et al. 2003). Therefore, the total DNA content or genome size obtained from the sum of all chromosomes was estimated as 1.77 $\pm$ 0.005 pg or 1,732,724 converted into base pairs (Mbp).

Analysis of variance was performed to detect the effects of chromosomal variability of DNA contents in chromosomes of *Haliotis rufescens*. Significant differences were detected among chromosome type ($P < 0.001$). However, the *posteriori* analysis using Tukey HSD test, showed statistical differences only among extreme chromosomes, specifically among chromosomes 1–4 and chromosomes 13–18 ($P < 0.05$). The mean DNA contents showed a significant increment from chromosome 18 to chromosome 1 ($P < 0.001$) (Fig. 6). The largest variability of chromosomal DNA contents was observed in chromosomes 2, 4, 8, 11 and 15.

The correlation between DNA content and chromosome length was performed to ascertain the relationship among chromosomal size and condensation level of DNA. The correlation value was statistically significant ($P < 0.001$) with r = 0.8783 (Fig. 7). The same analysis was carried out for the chromosomal DNA content and chromosome area. The correlation value was r = 0.9066 and statistically significant ($P < 0.001$) (Fig. 8). The numbers inside the chart represent the chromosome type.

DISCUSSION

For several decades chromosomes have been analyzed by traditional karyotyping, which depends on the analysis of characteristic banding patterns along the length of each chromosome. The major disadvantage of conventional cytogenetic banding methods is the limited resolution (Langer et al. 2004). Computerized chromosome analyses began mainly by analyzing mammal chromosomes during the 1960s (Carlson et al. 1963). Several advances, in theoretical and in applied disciplines have made it possible to develop various automated systems, that can be used for cytogenetic diagnostic purposes (Weierich et al. 2003). In plants, the chromosome image analyzing system (CHIAS), which uses a universal image analyzer, has been developed and applied in several studies (Fukui et al. 1998, Kato & Fukui 1998, Lee et al. 2004). The CHIAS allows the identification of small plant chromosomes based on their condensation pattern.

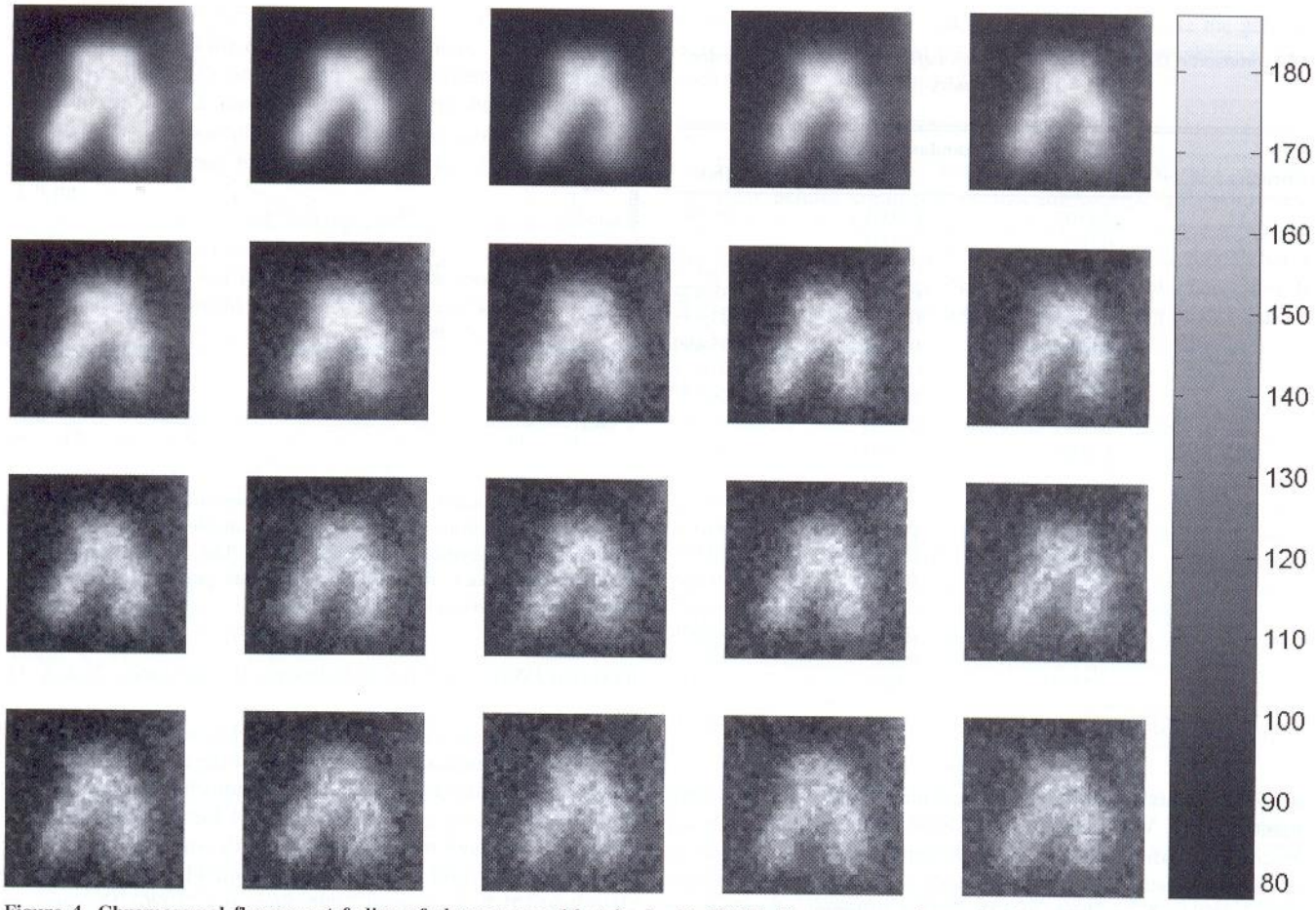

Figure 4. Chromosomal fluorescent fading of chromosome 16 stained with DAPI. The sequence shows the fluorescence fading period in a chromosome exposed to ultraviolet light. The color bar indicates 256 level of brightness or fluorescence intensity form 0–255.

In reference to cell DNA content estimation, several methods have been developed (Hardie et al. 2002). However, the main method applied to estimate the DNA contents in chromosomes has been so far flow cytometry. In flow cytometry, isolated chromosomes suspended in a fluorescent stain solution flow one at a time through a laser beam. The fluorescence signals resulting from laser excitation are measured for the chromosomes, yielding a frequency distribution of chromosomal fluorescence. The advantage of this method is related to the large number of chromosomes analyzed, providing high-precision population averages, that are not affected by cell-to-cell variations in chromosome condensation (Langlois et al. 1982).

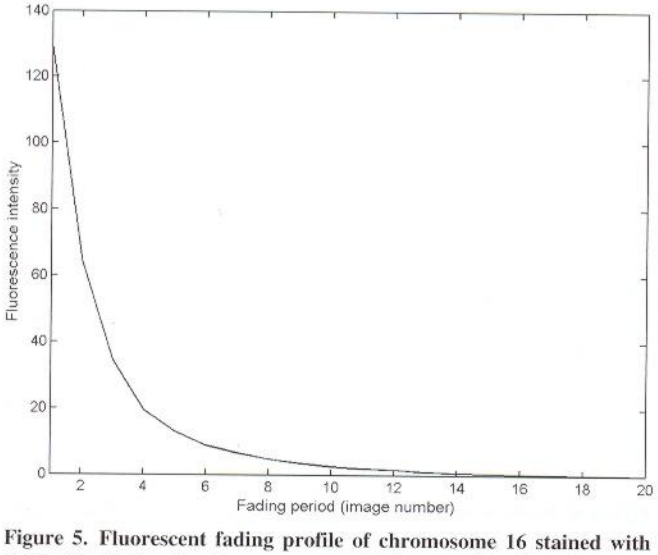

Figure 5. Fluorescent fading profile of chromosome 16 stained with DAPI. The fading function was generated by quantification of fluorescence intensity (FI). The area under the curve represents the integral fading.

The cytogenetic studies in invertebrates like molluscs are particularly problematic mainly because of their smaller chromosome size. However, several studies have been developed successfully, obtaining chromosomal banding and location by FISH of some genes of interest (Guo & Allen 1997, Zhang et al. 1999b, Vitturi et al. 2002, Gallardo-Escárate et al. 2005a). Nevertheless, flow karyotyping in molluscs showed problems caused by difficulties in obtaining pure cellular line cultures. In this context, this study represents an alternative method to estimate the chromosomal DNA contents by fluorescence image analysis. Our results showed that there is a positive correlation with their chromosome sizes ($P < 0.001$). Correlation values determined for chromosome length and area showed an improvement in the correlation value using chromosome area ($r = 0.8783$ and $r = 0.9066$ respectively). Possibly, this increase in r value could be because of condensation variation between chromosomes, and then the area measurement was a better indicator for chromosome size. According to Zhang et al. (1999a) the difference (percentage variation) among measurements of individual chromosomes was less than 5% in *Crassostrea*

TABLE 1.

Chromosome DNA content of *Haliotis rufescens* and its conversion into Mega base pairs (Mbp).

Chromosome	Mean DNA Content (pg)	Standard Deviation (pg)	Mbp*
1	0.1106	0.0045	108,201
2	0.1051	0.0098	102,752
3	0.1035	0.0053	101,175
4	0.1010	0.0093	98,824
5	0.0999	0.0077	97,655
6	0.0976	0.0072	95,490
7	0.0997	0.0089	97,474
8	0.0982	0.0099	96,087
9	0.0994	0.0063	97,243
10	0.1006	0.0094	98,393
11	0.0975	0.0104	95,319
12	0.0979	0.0085	95,757
13	0.0969	0.0075	94,784
14	0.0958	0.0087	93,690
15	0.0934	0.0090	91,355
16	0.0939	0.0076	91,825
17	0.0917	0.0077	89,640
18	0.0890	0.0060	87,056
Total	1.7717	0.0050	1,732,720

* Number of base pairs = mass in pg × 0.978 × 10^9 (Dolezel et al. 2003)

virginica, which accounted for technical variation (including manual error). Variation caused by biologic factors was analyzed by comparing different spreads of the same tissue type and spreads of different tissue types. The difference in relative lengths average was found to be as high as 9% among different spreads from individual embryos. In this sense, the difference found in our data could be largely derived from the continuous changes of chromosome morphology produced during the cell cycle. On the other hand, results of this study demonstrate that our measurement system is sensitive and capable of detecting minor differences among individual chromosomes. However, it was difficult to sort chromosomes of intermediate sizes using chromosomal DNA contents. Statistical analysis showed differences only among extreme chromosomes (1–4 and 13–18). This study shows the largest chromosomal DNA variability in following chromosomes: 2, 4, 8, 11 and 15.

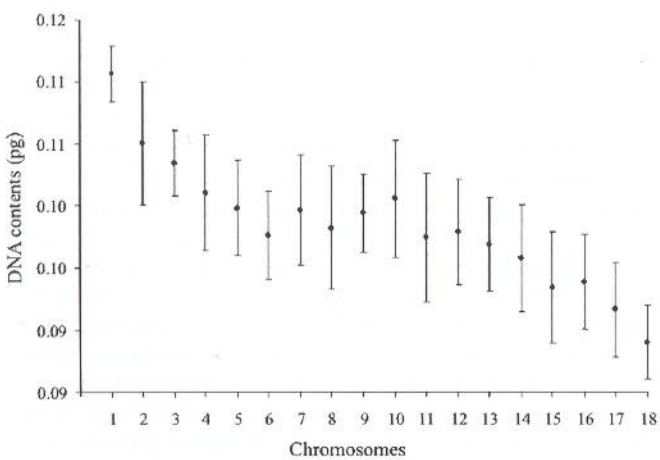

Figure 6. Chromosomal DNA contents in *Haliotis rufescens*. The mean DNA contents were obtained by fluorescence image analysis method. The bars represent 2 standard deviations.

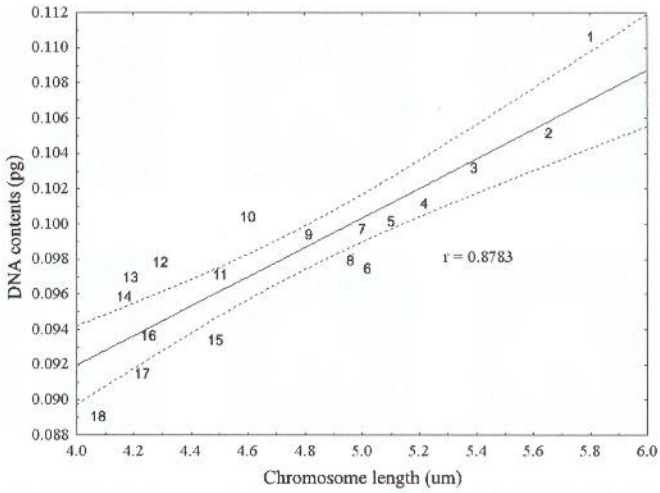

Figure 7. Correlation between the chromosomal DNA content and chromosome length (n = 18). The numbers inside represent the chromosome pair according to the karyotype. The linear equation was estimated by Fisher analysis. Discontinuous plotted line represents calculated standard error.

In reference to fluorescence fading method, this technique is based on the fluorescent decay lifetime of the fluorochrome when this is exposed to excitation light. The photochemical process underlying the fluorescence decay of DAPI has not yet been fully explained, although theories suggesting the involvement of oxygen, triplet states and protein denaturalization have been proposed (Hirschfeld 1979, Song et al. 1995, Song et al. 1996). However, to prevent retardation of fading in microscopy, several methods can be used to remove oxygen from the mounting medium. Furthermore it is feasible to increase the viscosity of the medium and avoid the oxygen diffusion (Johnson et al. 1982, Onoa et al. 2001). The point is to retard the diffusion of oxygen and consequently reduce the amount of oxidized fluorochromes. Our proposed method only used phosphate buffer saline (PBS) as mounting me-

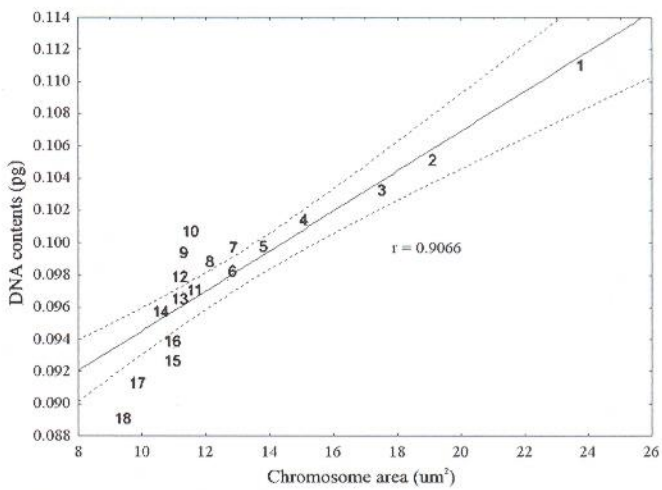

Figure 8. Correlation between chromosomal DNA content and chromosome area (n = 18). The numbers inside represent the chromosome pair according to the karyotype. Discontinuous plotted line represents calculated standard error.

dium, therefore the photochemical process is not modified. In this study we estimated the individual DNA content for each chromosome type (Table 1), and the total DNA content or genome size refers to the haploid amount of DNA. Our data show a genome size for *Haliotis rufescens* of 1.77 ± 0.005 pg. Hinigardner (1974) using classic techniques reported for this species a genome size of 1.8 pg.

We have described here a fluorescent imaging method for analyzing chromosome morphology and especially chromosomal DNA contents. To our knowledge, this is the first report of chromosomal DNA content in molluscs by image analysis. Furthermore, this methodology has been applied to estimate the genome size of two populations of the northern scallop *Argopecten purpuratus* (Gallardo-Escárate et al. 2005c).

ACKNOWLEDGMENTS

The authors thank Dr. Jaroslav Dolezel and Karin Lohrmann for their helpful comments on this manuscript. This study was supported by the Mexican National Council of Science and Technology (Project 36075-B and Project 33018-B). The first author is a CONICYT-BID (Chile) Ph.D. fellow and thanks Dirección de Telemática for the support received in the writing of this paper.

LITERATURE CITED

Arai, K. & N. Wilkins. 1986. Chromosomes of *Haliotis tuberculata* L. *Aquaculture* 58:305–308.

Carlson, L., T. Caspersson & G. Foley. 1963. The application of quantitative cytochemical techniques to the study of individual mammalian chromosomes. *Exp. Cell Res.* 31:589–594.

Dolezel, J., J. Bartos, H. Voglmayr & J. Greilhuber. 2003. Nuclear DNA content and genome size of trout and human. *Cytometry* 51A:127–128.

Dolezel, J., M. Kubalákavá, J. Bartos & J. Macas. 2004. Flow cytogenetics and plan genome mapping. *Chromosome Res.* 12:77–91.

Fujino, K., O. Sei-Ichi & H. Inayoshi. 1987. Temperature tolerance differences among normal diploid and triploid pacific abalones. *Nippon Suisan Gakkishi* 53:15–21.

Fukui, K., S. Nakayama, N. Ohmido, H. Yoshiaki & M. Yamabe. 1998. Quantitative karyotyping of three diploid Brassica species by imaging methods and localization of 45s rDNA loci on the identified chromosomes. *Theor. Appl. Genet.* 96:325–330.

Gallardo-Escárate, C., J. Álvarez-Borrego, M. A. del Río-Portilla, I. Cross, A. Merlo & L. Rebordinos. 2005a. Fluorescence in situ hybridization of rDNA, telomeric (TTAGGG)n and (GATA)n repeats in the red abalone *Haliotis rufescens* (Archaeogastropoda: Haliotidae). *Hereditas* 142:1–7.

Gallardo-Escárate, C., J. Álvarez-Borrego, M. A. del Río-Portilla & V. Kober. 2004. Karyotype of Pacific red abalone *Haliotis rufescens* (Archaeogastropoda: Haliotidae), using image analysis. *J. Shellfish Res.* 23:205–209.

Gallardo-Escárate, C., J. Álvarez-Borrego, V. Kober & M. A. del Río Portilla. 2005b. Relationship between DAPI-Fluorescent fading and nuclear DNA content: an alternate method to DNA quantification? *Journal of Fluorescence:* Submitted.

Gallardo-Escárate, C., J. Álvarez-Borrego, E. von Brand Skopnik & M. A. del Río-Portilla. 2005c. Genome size estimation in two populations of the northern scallop *Argopecten purpuratus* (Lamarck, 1879), using fluorescence image analysis. *J. Shellfish Res.* 24:55–60.

Gray, B., R. Zori, P. Mcguire & R. Bonde. 2002. A first generation cytogenetic ideogram for the Florida manatee (*Trichechus manatus latirostris*) based on multiple chromosome banding techniques. *Hereditas* 137:215–223.

Guo, X. & S. Allen. 1997. Fluorescence in situ hybridization of vertebrate telomere sequence to chromosome ends of the pacific oyster, *Crassostrea gigas* Thunberg. *J. Shellfish Res.* 16:87–89.

Hardie, D., R. Gregory & P. Hebert. 2002. From pixels to picograms: A beginners' guide to genome quantification by feulgen image analysis densitometry. *J. Histochem. Cytochem.* 50:735–749.

Hinigardner, R. 1974. Cellular DNA content of the Mollusca. *Comp. Biochem. Physiol.* 47A:447–460.

Hirschfeld, T. 1979. Fluorescence background discrimination by prebleaching. *J. Histochem. Cytochem.* 27:96–101.

Houtsmuller, A., J. Oud, M. Montijn, M. Worring, A. Smeulders & N. Nanninga. 2000. Chromosome no. 1 of *Crepis capillaris* shows defined 3D-shapes in mitotic prophase. *Chromosome Res.* 8:243–252.

Johnson, G., R. Davidson, K. McNamee, G. Russell, D. Goodwin & E. Holborow. 1982. Fading of inmunofluorescence during microscopy: a study of the phenomenon and its remedy. *J. Inmunol. Methods* 55:231–242.

Kato, S. & K. Fukui. 1998. Condensation pattern (CP) analysis of plant chromosomes by an improved chromosome image analyzing system, CHIAS III. *Chromosome Res.* 6:473–479.

Kudo, M., K. Arai & K. Fujino. 1991. Triploidization of *Halliotis diversicolor diversicolor*. *Nippon Suisan Gakkishi* 57:1263–1267.

Langer, S., K. Jurgen, I. Jentsch & M. Speicher. 2004. Multicolor chromosome painting in diagnostic and research applications. *Chromosome Res.* 12:12–15.

Langlois, G., L. Yu, J. Gray & A. Carrano. 1982. Quantitative karyotyping of human chromosomes by dual beam flow cytometry. *Proc. Natl. Acad. Sci. USA* 79:7876–7880.

Lee, J.-H., Y. Ma, T. Wako, L. C. Li, K.-Y. Kim, S.-W. Park, S. Uchiyama & K. Fukui. 2004. Flow karyotypes and chromosomal DNA contents of genus *Triticum* species and rye (*Secale cereale*). *Chromosome Res.* 12:93–102.

Levan, A., K. Fredga & A. Sandberg. 1964. Nomenclature of centromeric positions on chromosomes. *Hereditas* 52:201–220.

Lindberg, D. 1992. Evolution, distribution and systematics of Haliotidae. In: S. Shepherd, M. Tegner & S. Guzmán del Próo, editors. Abalone of the world, biology, fisheries and cultured. Oxford, USA: Fishing News Books. pp. 3–18.

Lucretti, S. & J. Dolezel. 1997. Bivariate flow karyotyping in broad bean (Vicia faba). *Journal of Cytometry* 28:236–242.

Macas, J., J. Dolezel, S. Lucretti, U. Pich, A. Meister, J. Fuchs & I. Schubert. 1993. Localization of seed storage protein genes on flow-sorted field bean chromosomes. *Chromosome Res.* 1:107–115.

Maldonado, R., A. Ibarra, J. Ramírez, S. Avila, J. Vázquez & L. Badillo. 2001. Induction of triploidy in pacific red abalone (*Haliotis rufescens*). *J. Shellfish Res.* 20:1071–1075.

Nakamura, H. 1985. A review of molluscan cytogenetic information based on the CISMOCH computerized index system for molluscan chromosomes, Bivalvia, Polyplacophora and Cephalopoda. *Venus Jpn. Journal Malacology* 44:193–226.

Oakes, F. & R. Ponte. 1996. Abalone market: opportunities for cultured abalone. *Aquaculture* 140:187–195.

Onoa, M., T. Murakamib, A. Kudoc, M. Isshikid, H. Sawadaa & A. Segawae. 2001. Quantitative comparison of anti-fading mounting media for confocal laser scanning microscopy. *J. Histochem. Cytochem.* 49: 305–312.

Patterson, C. 1969. Chromosomes of mollusks. Proceedings of symposium on mollusca. Marine Biology Association India. pp. 635–690.

Rodriguez-Juiz, A. M., M. Torrado & J. Méndez. 1996. Genome-size variation in bivalve molluscs determined by flow cytometry. *Mar. Biol.* 126:489–497.

Song, L., E. Hennink, I. Young & H. Tanke. 1995. Photobleaching kinetics of fluorescein in quantitative fluorescence microscopy. *Biophys. J.* 68: 2588–2600.

Song, L., C. Varma, W. Verhoeven & H. Tanke. 1996. Influence of the

triplet excited state on the photobleaching kinetics of fluorescein in microscopy. *Biophys. J.* 70:2959–2968.

Thiriot-Quiévreux, C. 1994. Advances in cytogenetics of aquatic organisms. In: A. Beaumont, editor. Genetics and evolution of aquatic organisms. London: Chapman and Hall. pp. 369–388.

Trask, B. 2002. Human cytogenetics: 46 chromosomes, 46 years and counting. *Nature* 3:769–778.

Uozu, S., N. Ohmido, H. Ohtsubo, E. Ohtsubo & K. Fukui. 1997. Repetitive sequences: cause for variation in genome size and chromosome morphology in the genus *Oryza. Plant Mol. Biol.* 35:791–799.

Vitturi, R., M. Colomba, L. Castriota, A. Beltrano, A. Lannino & N. Volpe. 2002. Chromosome analysis using different staining techniques and fluorescent in situ hybridization in *Cerethium vulgatum* (Gastropoda: Cerithiidae). *Hereditas* 137:101–106.

Weierich, C., A. Brero, S. Stein, J. von Hase, C. Cremer, T. Cremer & I. Solovei. 2003. Three-dimensional arrangements of centromeres and telomeres in nuclei of human and murine lymphocytes. *Chromosome Res.* 11:485–502.

Zhang, G., Z. Wang, Y. Chang, Y. Song, Y. Ding, Y. Wang & R. Wang. 1998. Triploid induction in the pacific abalone *Haliotis discus hannai* ino by 6-dimethylaminopurine and the performance of triploid juveniles. *J. Shellfish Res.* 17:783–788.

Zhang, G., G. Yu, R. Cooper & T. Tiersch. 1999a. High-resolution analylsis of karyotypes prepared from different tissue of the Easter oyster *Crassostrea virginica. J. Shellfish Res.* 18:115–120.

Zhang, Q., G. Yu, R. Cooper & T. Tiersch. 1999b. Chromosomal location by fluorescence *in situ* hybridization of the 28s ribosomal RNA gene of the Eastern oyster. *J. Shellfish Res.* 18:431–435.